Crossover from Bose-Einstein Condensed Molecules to Cooper Pairs by Using Feshbach Resonance

Shu-Wei Chang

Department of Electrical and Computer Engineering,

University of Illinois at Urbana-Champaign, Urbana, IL 61801, USA

(Dated: May 6, 2004)

Abstract

At low temperature, fermionic atoms can either condense into a Bose-Einstein condensate (BEC) by forming bosonic molecules or be loosely paired to form Cooper pairs described by Bardeen, Cooper, and Schrieffer's (BCS) microscopic theory. Experimentalists have claimed the observation of the intermediate regime between BEC and BCS limits by tuning the scattering length with the aid of Feshbach resonance. In this report, we will discuss the idea of using Feshbach resonance to achieve the crossover. Some many-body formulation concerning this crossover will be briefly introduced, but not in detail. The experimental results will be our main concerns and addressed in this report.

I. INTRODUCTION

After the successful demonstrations of Bose-Einstein condensation (BEC) of atomic gas,[1, 2], the cooling down of atomic Fermi gas has also been achieved recently.[3, 4] Unlike bosonic atoms, fermionic atoms cannot condense into a single state due to anti symmetrization of the macroscopic wave function. However, two fermionic atoms can be converted into a bosonic molecule and condense into a BEC again.

Whether two fermionic atoms can form a bosonic molecule is closely related to the two-body physics of the atoms. The sign of the s-wave scattering length between two identical fermionic atoms in *different internal quantum states*, called an *open channel*, determines whether the effective interaction in that channel between two fermions is repulsive or attractive at low temperature.[5] The sign of the s-wave scattering length has a close connection with the near-by energy of the bound state in a *closed* channel of which threshold energy is higher than that of the open channel. For fermionic atoms with the same internal quantum states, the s-wave scattering cross section disappears due to anti-symmetrization of wave functions, and one has to consider scattering lengths due to, for example, p-wave scattering. Experimentally, it will be more efficient to observe the change of the s-wave scattering length in an open channel characterized by the scattering of the atoms with different internal quantum numbers.[6, 7] However, if the physical environment favors the atoms of a single internal quantum state, issues on p-wave scattering such as the analogy of p-wave pairing in superconductivity then can be discussed.[8]

For atoms, the s-wave scattering length can be controlled by mechanisms such as the interaction of magnetic moments with magnetic field[9] or Raman transition induced by lasers.[10, 11] In either case, the energy of the bound state in the closed channel is swept across the threshold energy of the open channel. It is possible to change the sign of the scattering length and thus the property of the effective interaction. For fermionic atoms, the controllability of the scattering length enables the formation of a correlated atom pair in one limit and a tightly-bound molecule in the other, as will be discussed in the next section. Experimentally, it is interesting to ask what happens to the pair of fermionic atoms at the crossover between the two limits. Theoretically, it can also provide an analogue test for one of the candidate theories of high temperature superconductivity, originated from Nozières and Schmitt-Rink by considering electron pairs resonant with the molecular state.[12]

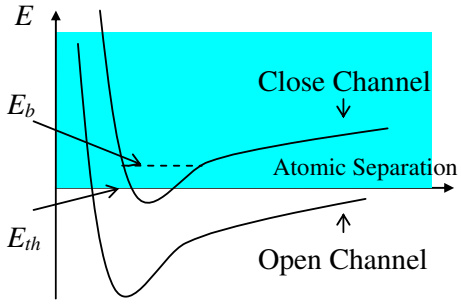

FIG. 1: Feshbach resonance of a quasi-bound state with the open channel. E_b is the resonant energy of the quasi-bound state. E_{th} is the threshold energy of the open channel. The blue part indicates the continuum of the open channel.

II. FESHBACH RESONANCE

Feshbach is first discussed in nuclear physics.[13] In this section, emphasis will be put on the Feshbach resonance using magnetic field. More details can be found in Ref. [5].

For fermionic atoms, Feshbach resonance is the change of the scattering length in an open channel due to the coupling to a bound state in the closed channel. The state in the closed channel will be a true bound state if either there is no coupling to the open channel, or the energy of the state lies below the threshold energy of the open channel. On the other hand, if the state has an energy lying in the continuum of the open channel and exhibits a finite coupling to the open channel, it should be called a *quasi-bound state* since it is not a true bound state. A quasi-bound state exhibits some sort of energy resonance just as a bound state but is characterized by a finite decay width due to the coupling to the open channel. Fig. 1 shows the Feshbach resonance of a quasi-bound state coupling to the open channel.

Write the general wave function $|\Psi>$ as a superposition of the part in the open channel $|\Psi_1>$ and the part in the closed channel $|\Psi_2>$. The two parts are orthogonal to each other: $<\Psi_2|\Psi_1>=0$. The Hamiltonian describing both open and closed channels is denoted as H. Also, write the projection operator to the open and closed channels as P_1 and P_2. We define various projected Hamiltonians as

$$H_{ij} = P_i H P_j, \qquad i,j = 1,2 \tag{1}$$

After a close look, the effective Hamiltonian H_{eff} describing the open channel is written as

$$H_{eff}|\Psi_1>=\Big[H_{11}+H_{12}(E-H_{22}+i\delta)^{-1}H_{21}\Big]|\Psi_1>=E|\Psi_1> \tag{2}$$

where δ is a small number. We further write the projected Hamiltonian H_{11} as $H_{11}=H_0+U$ where H_0 is the noninteracting part of the Hamiltonian H_{11}. The interaction term U_{eff} in the effective Hamiltonian H_{eff} is

$$U_{eff}=U+H_{12}(E-H_{22}+i\delta)^{-1}H_{21} \tag{3}$$

The effective s-wave scattering length is evaluated from equation (3) by Born's approximation for the zero momentum state $|\varphi_0>$ of the open channel. The energy of the state $|\varphi_0>$ is just the threshold energy E_{th} of the open channel. Denote a complete set of the eigenstates of the projected Hamiltonian H_{22} as $\{|\phi_n>, n=1,2,...\}$ with eigenenergies $\{E_n\}$. Due to the fact that $H_{12}=H_{21}^{\dagger}$ and the completeness relation $\mathbf{1}=\sum_n|\phi_n><\phi_n|$ in the closed channel, the s-wave scattering length a_s of this open channel can be written as

$$\begin{aligned} a_s &= \frac{m_r}{4\pi\hbar^2}<\varphi_0|U_{eff}|\varphi_0> \\ &= \overbrace{\frac{m_r}{4\pi\hbar^2}<\varphi_0|U|\varphi_0>}^{a_{s,1}}+\frac{m_r}{4\pi\hbar^2}\sum_n\frac{|<\phi_n|H_{21}|\varphi_0>|^2}{E_{th}-E_n+i\delta} \\ &= \underbrace{\left[a_{s,1}+\frac{m_r}{4\pi\hbar^2}\sum_{n,E_n\neq E_b}\frac{|<\phi_n|H_{21}|\varphi_0>|^2}{E_{th}-E_n+i\delta}\right]}_{a_{nr}}+\frac{m_r}{4\pi\hbar^2}\frac{|<\phi_b|H_{21}|\varphi_0>|^2}{E_{th}-E_b+i\delta} \end{aligned} \tag{4}$$

where $a_{s,1}$ denotes the s-wave scattering length in the open channel; $|\phi_b>$ is the (quasi-) bound state with energy E_b nearest to the threshold energy E_{th}; and a_{ns} is the nonresonant part of the s-wave scattering length. The contribution from the state $|\phi_b>$ is separated from the summation since it is the most significant. The denominator $E_{th}-E_b$ in equation (4) is a function of the applied magnetic field B. Denote the internal quantum numbers labeling the two atoms in the open channel as α and β where $\alpha\neq\beta$. Near a particular magnetic field B_0, the denominator can be expanded as

$$E_{th}-E_b\approx(\mu_b-\mu_\alpha-\mu_\beta)(B-B_0) \tag{5}$$

where μ_b, μ_α, and μ_β are the magnetic moments of the (quasi-) bound state and the states labeled by internal quantum numbers α and β. If the nonresonant s-wave scattering length a_{nr} does not vary too much with the magnetic field, equation (4) can be written as

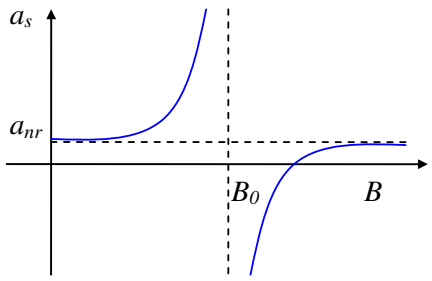

FIG. 2: S-wave scattering length as a function of magnetic field.

$$\begin{aligned} a_s &= a_{nr}(1 + \frac{\Delta B}{B - B_0 + i\delta_B}) \\ \Delta B &= \frac{m_r}{4\pi\hbar^2 a_{nr}} \frac{|<\phi_b|H_{21}|\varphi_0>|^2}{\mu_b - \mu_\alpha - \mu_\beta} \end{aligned} \tag{6}$$

where δ_B is an infinitesimal quantity. A typical s-wave scattering length as a function of the magnetic field is shown in Fig. 2 for $a_{nr} > 0$ and $\Delta - B > 0$. The scattering length diverges to plus and minus infinities as the magnetic field tends to B_0^- and B_0^+. Examples include the s-wave scattering length for $|F = 9/2, m_F = -9/2> + |F = 9/2, m_F = -7/2>$ of ^{40}K[6, 14, 15] and so on. Also, this scattering is an *elastic* one since the kinetic energy is not lost during the scattering.

If the threshold energy E_{th} is slightly larger than E_b, the s-wave scattering length is positive. Although the effective interaction potential corresponding to this positive elastic scattering length is repulsive, two fermionic atoms can form a molecule when the magnetic field is swept downward across the magnetic field B_0. In this case, it is possible to form BEC from these bosonic molecules. The energy difference between the two atoms and molecule is brought away by three-body processes instead of the s-wave two-body inelastic scattering which is believed to be absent.[8, 16–19] However, the molecules produced in this way are usually highly vibrationally excited. The deexcitation of these molecules will cause significant inelastic scattering, and the loss rate of these molecules is high.[6, 7, 20] On the other hand, for the negative scattering length (attractive interaction), atoms in the open channel cannot form a stable molecule described by a true bound state. They can interact via the quasi-bound state and form a correlated pair, or may be viewed as molecules with *finite* lifetime. This regime should be described by a generalized Bardeen, Cooper, and Schrieffer's (BCS) theory instead of BEC. Typically, the atoms in this regime have lower loss rate than the molecules in the other side of the resonance. [6, 7, 20]

III. ON THE MANY-BODY ASPECTS

In atomic gases, the presence of quasi-bound state is easily modeled by adding a coupling term to a molecular state in the BCS Hamiltonian for fermionic atoms.[21–23]

$$\begin{aligned} H &= \sum_k \epsilon_k (a^\dagger_{k,\uparrow} a_{k,\uparrow} + a^\dagger_{k,\downarrow} a_{k,\downarrow}) + U_{bg} \sum_{k_1+\ldots+k_4=0} a^\dagger_{k_1,\uparrow} a^\dagger_{k_2,\downarrow} a_{k_3,\downarrow} a_{k_4,\uparrow} \\ &\quad + g \sum_{k,q} (b^\dagger_q a_{q/2+k,\uparrow} a_{q/2-k,\downarrow} + b_q a^\dagger_{q/2-k,\downarrow} a^\dagger_{q/2+k,\uparrow}) + \sum_q (\nu + E_q) b^\dagger_q b_q \end{aligned} \tag{7}$$

where a (b) and $a^\dagger$ ($b^\dagger$) are the annihilation and creation operators of atoms (molecules); ϵ_k and E_q are the the kinetic energies of atoms and molecules; $\uparrow$ and $\downarrow$ are *pseudo spins* indicating the two different internal quantum states; U_{bg} is the background attractive potential between atoms; μ is the bound-state energy relative to the threshold of the open channel due to the magnetic field; and g describes the exchange between atoms and molecules. This Hamiltonian describes the superfluidity of Fermi atoms in the BEC limit, BCS limit, and the intermediate regime. The change of the scattering length is not obvious in equation (7) but is implicitly included due to the coupling constant g. This model is a more rigorous picture than the two-body one in the previous section because the corresponding effective theory fails if the scattering length is large near the resonance.

Instead of going through the mathematical details, we only mention a few results of key calculations. The detailed treatments of this Hamiltonian or its mutants for atomic Fermi gas can be found in literatures.[21–25]

Fig. 3 shows the critical temperature, the chemical potential, and the fractions of atoms and molecules at the emergence of superfluidity as a function of the bound-state energy.[23] This result is obtained numerically by self-consistently solving the gap equation and the conservation of particle number.

$$\begin{aligned} 1 &= (-U_{bg} + \frac{g^2}{\nu - 2\mu}) \sum_k \frac{\tanh[\beta(k^2/2m - \mu)/2]}{2(k^2/2m - \mu)} \\ N &= 2\sum_k \frac{1}{e^{\beta(k^2/2m-\mu)}+1} + 2\sum_k \frac{1}{e^{\beta(k^2/4m+\nu-\mu)}+1} - \frac{1}{\beta}\sum_q \frac{\partial}{\partial\mu} \ln[1 - \chi(q, i\omega)] \end{aligned} \tag{8}$$

where μ is the chemical potential; N is the total particle number; and $\chi(q, i\omega)$ is a correction function describing the number fluctuations of atoms and molecules. In Fig. 3(a), the solid line shows the critical temperature calculated from equation (8). The dash line is a calculation by substituting equation (6) into U_{bg} and solving the BCS gap equation. The

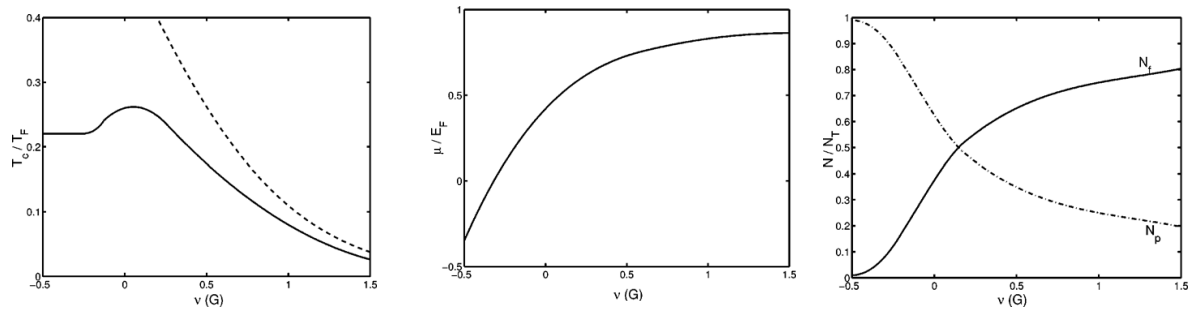

(a) (b) (c)

FIG. 3: Physical quantities at the emergence of superfluidity as a function of the bound-state energy. (a) Critical temperature. Solid line is the result from equation (8). Dash-line is the result from the reduced BCS theory. (b) Chemical Potential. (c) Fractions of atoms and molecules. Solid line is the fraction of the fermions while the dot-dash line is the pair fraction. After Ref. [23]

critical temperature calculated from simple BCS gap equation diverges at the resonance because the interaction energy U_{bg} calculated in this way diverges to minus infinity. The solid line matches well with the simple BCS theory when the bound-state energy is above the threshold. On the other hand, it approaches the critical temperature predicted by BEC theory at the other limit. As the bound-state energy is tuned downward from the BCS side toward the resonance, the critical temperature increases, which makes this model a candidate for high-temperature superconductivity. There is an optimized critical temperature close to the threshold energy. This critical temperature is around 0.26 T_F, where T_F is the Fermi temperature of the atoms without any molecules. Similarly in Fig. 3(b), the chemical potential is also a smooth connection between the two limits. In the BCS limit, the chemical potential approaches that of the Fermi gas at critical temperature. In the BEC limit, the chemical potential will tend to one half of the bound-state energy. This is an analogy to that the chemical potential of pure bosons approach their ground energy as BEC occurs. Fig. 3(c) shows the fractions of fermionic atoms and atom pairs. The fraction of fermions approach zero as the system goes deep into BEC limit while the pair fraction shows the opposite trend. The atom pairs resemble Cooper pairs above the resonance but are like molecules below the resonance.

The calculation stated above is only related to the physical quantities when the superfluidity phase occurs. The question on whether there is a transition between BEC and

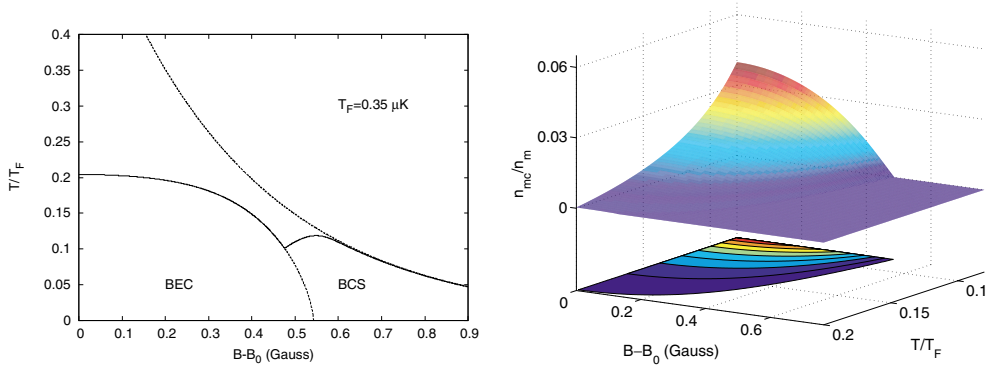

(a) (b)

FIG. 4: (a) The phase diagram of BCS-BEC transition. The upper dash line is the critical temperature calculated from simple BCS theory. The lower dash line is the BCS-BEC boundary. (b) The fraction of BEC condensate as a function of the magnetic field and temperature. After Ref. [26]

BCS limits, i.e., a boundary between BEC and BCS regimes in the phase diagram shown in Fig. 4(a), is also interesting.[26] At zero temperature, write the pair wave function as the superposition of the open and closed-channel wave functions $\chi_m(x,x')$ and $\chi_{aa}(x,x')$,

$$\sqrt{Z(B)}\chi_m(x,x')|\text{closed} > +\sqrt{1-Z(B)}\chi_{aa}(x,x')|\text{open} > \tag{9}$$

the question of BCS-BEC crossover becomes whether we can find a critical magnetic field $B_c(T=0)$ such that the parameter $Z(B<B_c(T=0))=1$ and $Z(B>B_c(T=0))=0$. At finite temperatures less than the critical temperature, the question becomes whether there is a critical magnetic field $B_c(T)$ below which molecules begin to condense into the molecular ground state, i.e., $n_{m,BEC}(B<B_c(T),T)/n_m(B<B_c(T),T)>0$. We first note that the critical temperature calculated in Ref. [23] has a different shape from that calculated in Ref. [26]. It may be a result of different approximations used in the calculations. Fig. 4(b) shows the BEC fraction as a fraction of the magnetic field and temperature. At a given temperature, there is a critical magnetic field $B_c(T)$ where the BEC condensate emerges. These critical magnetic fields $B_c(T)$ deviate from B_0 predicted by simple two-body physics. A simple argument about these deviations is that molecules, though with a finite lifetime in the BCS regime, will emerge from atomic Fermi sea when the shifted ground state energy of molecules due to the coupling is roughly twice the chemical potential of the system. This early formation of the molecular condensate before the exact resonance makes the superfluidity at this crossover unusual.

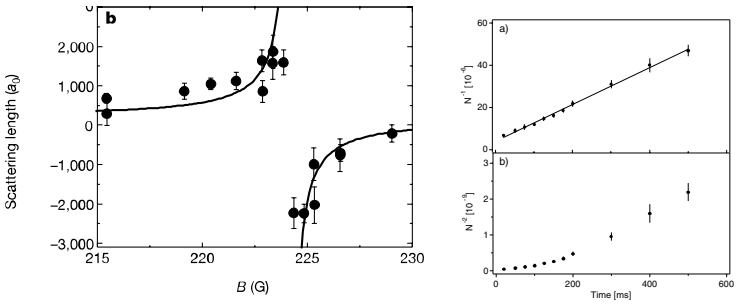

(a) (b)

FIG. 5: (a) The scattering length of ^{40}K. (b) The inelastic scattering rate of ^{6}Li. The upper and lower figure are the inverse and inverse square of the population as a function of time, indicating the two-body and three-body processes. After Ref. [9, 14].

IV. EXPERIMENTS ON BCS-BEC CROSSOVER

Most of the experiments on BCS-BEC crossing are aimed at fermionic atoms ^{6}Li and ^{40}K.[2, 4, 6, 7, 9, 14, 15, 17–19] For ^{6}Li, two hyperfine states $|1/2, 1/2>$ and $|1/2, -1/2>$ are used while for ^{40}K, two states $|9/2, -7/2>$ and $|9/2, -9/2>$ are used.

Fig. 5(a) shows the elastic scattering length of ^{40}K as a function of magnetic field.[14] The Feshbach resonance of ^{40}K takes place at 224.18 G. The magnitude of the scattering length is obtained from the extraction of rethermalization time by heating the atomic gas when modulating the power of the optical trap.[9] The sign of the scattering length is obtained by measuring the mean-filed shift of the transition $|9/2, -9/2> \longrightarrow |9/2, -5/2>$.[15] The change of the scattering length is very significant as the magnetic field sweeps across the resonance frequency, indicating the ability to control the effective interaction between ^{40}K atoms. Fig. 5(b) shows the inelastic loss rate of ^{6}Li at 680 G.[17] There are two Feshbach resonance peaks for ^{6}Li–550 G and 822 G. The resonance at 822 G has a very broad lineshape, and thus the inelastic scattering at 680 G is believed to be greatly influenced by this resonance. The upper plot of Fig. 5(b) shows the inverse of the number of particles remaining in the trap as a function of time. The nearly linear behavior seems to imply that the two-body inelastic process dominates in the time scale observed. The lower plot shows the inverse square of the population as a function of time. The three-body process will dominate over the two-body process only when the population is high. The small linear part at time close to zero thus indicates the three-body process. However, the inelastic two-body

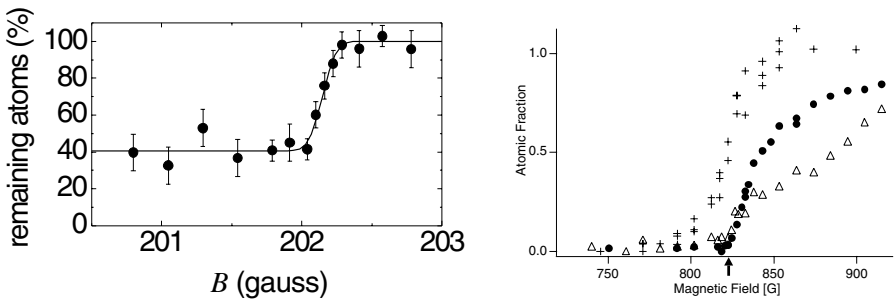

(a) (b)

FIG. 6: (a) The fraction of ^{40}K atoms as a function of the magnetic field. (b) The fraction of ^{6}Li atoms as a function of the magnetic field. Cross: initial ramp-down speed=30 G/μs; circle: linear ramp-down at 100 G/ms; triangle: linear ramp-down at12.5 G/ms. After Ref. [7, 19].

loss is believed to be suppressed. In Ref. [17], the author thus attributed the observed loss rate to the three-body process simultaneously accompanying by the temperature change.

Fig. 6(a) and (b) show the fractions of fermionic atoms ^{40}K at 224.18 G[19] and ^{6}Li at 822 G[7] as a function of the magnetic field. In either case, the measurement begins from the BEC side where bound molecules exist. The magnetic field is first swept up to a given value. If the given magnetic field exceeds the resonant magnetic field, the molecules will dissociate. During the sweeping which takes about more than ten milliseconds, the molecular or atomic gas will expand so that the density of the gas is diluted. This action is performed to avoid the unwanted interference from many-body effects and the reformation of molecules at successive stage.[6, 7] After the expansion, the magnetic field is fast ramped down to zero. The fraction of the atoms is then obtained at zero field by optical image method which only detects the atoms because the transition of molecules does not match the frequency of the incident light.[6, 14, 27] From Fig. 6(a) and (b), the fraction of atoms greatly increase as the given magnetic field goes above the resonance, indicating the absence of molecules. Also, in Fig. 6(b), the fraction of atoms corresponding to different speeds of ramping the magnetic field down to zero are shown. This ramp-down speed has to be carefully chosen because the resonant field B_0 obtained in this way will shift due to the ramp-down speed.[7] However, the ramp-down speeds used in the experiments do not significantly change the resonant field.

Fig. 7(a) and (b) show the fraction of the condensate of *pair atoms* (This term should

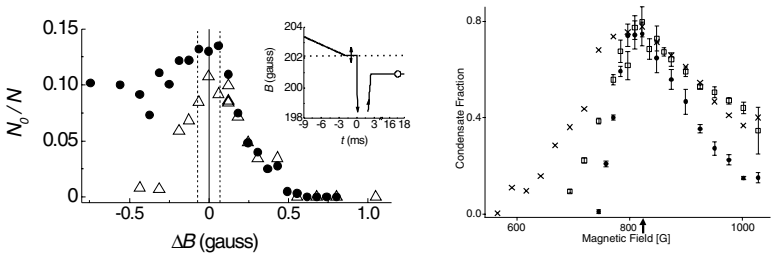

(a) (b)

FIG. 7: (a) The decay of $^{40}K_2$ condensate fraction. Circle: 2 ms hold time; triangle: 30 ms hold time (b) The decay of $^6Li_2$ condensate fraction. Cross: 2 ms hold time; square: 100 ms hold time; circle: 10 s hold time. After Ref. [6, 7].

stand for BEC molecules in the BCS side although its real meaning is a bit ambiguous in these papers.) as a function of magnetic field for ^{40}K[6] and ^{6}Li.[7] Unlike Fig. 6(a) and (b), the initial magnetic field is set at the BCS side and than brought slowly to a given magnetic field to avoid the enhanced loss out of the optical trap due to rapid sweeping. No expansion of atomic gas takes place at this stage. Furthermore, sometimes it is even necessary to in crease optical power to enhance the confinement of the atomic gas.[7] The atomic gas is held there for a period of time which is variable in the experiments. After the hold period, the trap is turned off to allow the gas to expand. Simultaneously[6] or immediately after the expansion,[7] the magnetic field is soon turned off. Unlike the experiments mentioned previously, the atom in the gas will be adiabatically turned into molecules due to high density. The fraction of molecular BEC condensate, which is assumed to be invariant before and after the turn-off by some subtle argument, is then measured by mapping out the zero momentum component[7] or Thomas-Fermi profile of the molecules.[6]

In Fig 7 (a) and (b), the fraction of the condensate decays as the hold time increases. As mentioned in section II, the formation of molecules by sweeping the magnetic field across the resonance creates vibrationlly-excited molecules. The deexcitation of these molecules will cause the inelastic scattering and quench the fraction od the BEC condensate. The longer the hold time is, the more thorough the quenching is. It accounts why significant decay is observed at longer hold time. Close to the resonance and in the BCS side, the condensate decays slowly while it decays faster farther away from the resonance in the BEC side because the molecules are more tightly-bound. The extra bound energy has to be converted into

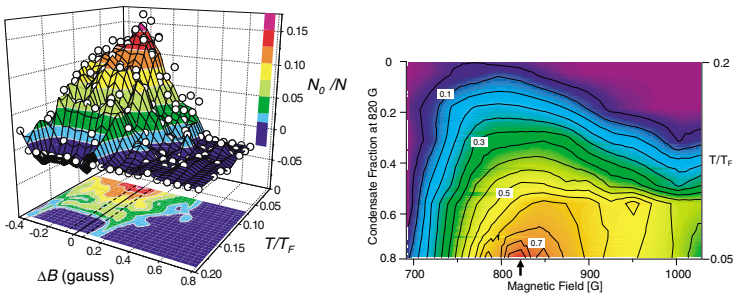

(a) (b)

FIG. 8: The fractions of (a) $^{40}K_2$ BEC condensate and (b) $^6Li_2$ BEC condensate as a function of the magnetic field and temperature. After Ref. [6, 7].

kinetic energy and reduces the condensate fraction.[28]

The argument that the condensate fraction measured in this way is just the condensate fraction before the turn-off of the magnetic field is subtle. This argument will lead to the conjecture that the BEC is present in the BCS side.[26] The argument is based on two assumptions. The first one is that no BEC condensate is created when the magnetic field drops to zero.[14] The second one is that slightly-correlated atoms tend to randomly pick up a neighboring atom to form a molecule. Molecules formed in this way have finite momenta and do not belong to the condensate. Therefore, the original condensate will be directly projected to the condensate at zero magnetic field.[7] The condensate fraction as a function of magnetic field and temperature for a given number of atoms is also measured.[6, 7] Fig. 8 (a) and (b) show the corresponding three-dimensional and contour plots for $^{40}K_2$ and $^6Li_2$ molecules. Fig. 8 (a) can be directly compared with Fig. 4 (b) since this figure is an attempt to fit the experimental data.

V. CONCLUSION

We have briefly surveyed the recent experiments on BEC-BCS crossover. Instead of going into complicated calculations of many-body dynamics, we only look into those related to thermal equilibrium. The interesting point of the cold fermionic atoms is the capability of tuning the scattering length by magnetic field. BEC and BCS types of superfluidity can thus be achieved in the same system by tuning this controllable parameter. Further, an interesting regime of superfluidity between BEC and BCS has been opened. More future work has to be devoted to explore the properties of the superfluidity phase in the regime.

[1] M. H. Anderson et al., Science **269**, 198 (1995).

[2] K. B. Davis et al., Phys. Rev. Lett. **75**, 3969 (1995).

[3] F. A. van Abeelen, B. J. Verhaar, and A. J. Moerdijk, Phys. Rev. A **55**, 4377 (1997).

[4] B. DeMarco and D. S. Jin, Science **285**, 1703 (1999).

[5] C. Pethick and H. Smith, *Bose-Einstein Condensation in Dilute Gases* (Cambridge University Press, Cambridge, UK, 2002), 1st ed.

[6] C. Regal, M. Greiner, and D. Jin, Phys. Rev. Lett. **92**, 040403 (2004).

[7] M. W. Zwierlein et al., Phys. Rev. Lett. **92**, 120403 (2004).

[8] J. L. Bohn, Phys. Rev. A **61**, 053409 (1999).

[9] T. Loftus et al., Phys. Rev. Lett. **88**, 173201 (2002).

[10] F. K. Fatemi, K. M. Jones, and P. D. Lett, Phys. Rev. Lett. **85**, 4462 (2000).

[11] S. Kokkelmans, H. M. J. Vissers, and B. J. Verhaar, Phys. Rev. Lett. **63**, 031601(R) (2001).

[12] P. Nozières and S. Schmitt-Rink, J. Low Temp. Phys. **59**, 195 (1985).

[13] H. Feshbach, Ann. Phys. **19**, 287 (1962).

[14] C. A. Regal, C. Ticknor, J. L. Bohn, and D. S. Jin, Nature (London) **424**, 47 (2003).

[15] C. A. Regal and D. S. Jin, Phys. Rev. Lett. **90**, 230404 (2003).

[16] V. A. Yurovsky and A. Ben-Reuven, Phys. Rev. A **60**, R765 (1999).

[17] K. Dieckmann et al., Phys. Rev. Lett. **89**, 203201 (2002).

[18] C. A. Regal, C. Ticknor, J. L. Bohn, and D. S. Jin, Phys. rev. Lett. **90**, 053201 (2003).

[19] C. A. Regal, M. Greiner, and D. S. Jin, Phys. Rev. Lett. **92**, 083201 (2004).

[20] K. E. Strecker, G. B. Partridge, and R. G. Hulet, Phys. Rev. Lett. **91**, 080406 (2003).

[21] M. Holland et al., Phys. Rev. Lett. **87**, 120406 (2001).

[22] Y. Ohashi and A. Griffin, Phys. Rev. Lett. **89**, 130402 (2002).

[23] J. N. Milstein, S. Kokkelmans, and M. J. Holland, Phys. Rev. A **66**, 043604 (2002).

[24] M. Mackie, K.-A. Suominen, and J. Javanainen, Phys. Rev. Lett. **89**, 180403 (2002).

[25] P. Naidon, Grancoise, and Masnou-Seeuws, Phys. Rev. A **68**, 033612 (2003).

[26] G. M. Falco and H. T. C. Stoof, Phys. Rev. Lett. **92**, 130401 (2004).

[27] M. W. Zwierlein et al., Phys. Rev. Lett. **91**, 250401 (2003).

[28] J. Cubizolles et al., Phys. Rev. Lett. **91**, 240401 (2003).